A more efficient microgrid operation through the integration of probabilistic solar forecasts

Faly H Ramahatana, Josselin Le Gal La Salle, Philippe Lauret, Mathieu David

A more efficient microgrid operation through the integration of probabilistic solar forecasts

Faly Ramahatana[a], Josselin Le Gal La Salle[a], Philippe Lauret[a], Mathieu David[a]

[a] *University of La Réunion - PIMENT laboratory, 15, avenue René Cassin, Saint-Denis, 97715, Reunion*

Abstract

This work proposes a methodology based on the probabilistic dynamic programming (PDP) to integrate operational probabilistic forecasts of a photovoltaic (PV) plant into the optimization of the day-ahead schedule of an energy storage system (ESS). The proposed approach is tested on a microgrid based on a real educational building, a PV farm and Li-ion batteries. The objective is to minimize the operating cost of the microgrid. The operational day-ahead forecasts are derived from the Ensemble Prediction System (EPS) provided by a well-known Numerical Weather Prediction (NWP) model. Contrary to the classical use of deterministic forecasts, we demonstrate that the integration of the probabilistic forecasts in the optimization process leads to a more efficient microgrid management and to a reduction of up to 38% of the operating costs. Besides, it is shown that the non linearity resulting from the power dependency of the efficiency of the inverters must be taken into account in order to yield relevant optimization results.

Keywords:
Solar energy, probabilistic forecast, microgrid, unit commitment, probabilistic dynamic programming

*corresponding author

Email address: faly.ramahatana-andriamasomanana@univ-reunion.fr (Faly Ramahatana)

1. Introduction

For the grid manager, the unit commitment (UC) is an important operation for grid and microgrid management. The objective of the UC is to schedule the operation of the production units with a minimum cost and at a reliable level. The optimization of unit commitment is extensively studied in the literature, as described by Saravanan et al. [1] and by Abdou and Tkiouat [2]. Indeed, numerous optimization techniques are proposed to solve the unit commitment problem, like DP (Dynamic Programming), MILP (Mixed Integer Linear Programming), SP (Stochastic Programming), RO (Robust Optimization), QP (Quadratic Programming) and others. The use of those optimization methods depends on the system characteristics, the constraints and the objectives of the grid manager. For example, considering worst-case operating scenarios, Jiang et al. [3] used a RO (Robust Optimization) to solve the UC problem.

With the seek of decarbonization and energy supply security, the current trend is on increasing renewable energy productions in the energy mix. Wind and solar energy are abundant RES (Renewable Energy Source) and the associated conversion systems, such as photovoltaics (PV) or wind turbines, are mature technologies. But those intermittent RES are highly variable in both space and time. In this work, we will focus on the PV production. Indeed, this technology is currently the most affordable RES and also the most used worldwide [4]. Furthermore, unlike conventional generators, intermittent energy plants are non-dispatchable production units. These two characteristics of intermittent RES result in an important uncertainty of their generation. As a consequence, the increase of the intermittent renewables share in the production mix adds more complexity to the grid management, especially to take these new uncertainties into account in the UC problem. To solve the UC problem in the presence of uncertainty, two complementary approaches exist: the use of forecasts and the stochastic optimization called stochastic UC.

First, the use of point forecast, which gives a single value to predict a future level of power generation and which assumes a deterministic dynamic of the system, allows improving the scheduling. For example, Yang et al. [5] show that the use of PV and wind forecasts lead to better decisions in the UC problem. A lot of forecasting techniques exists to predict the future production of solar renewables. Diagne et al. [6], Antonanzas et al. [7] or Sobri et al. [8] propose reviews of solar forecasting methods and they highlight that

the suitable techniques depend on the spatial and temporal scales.

In the literature, one can find several works dealing with the integration of deterministic forecasts of renewable power generation in UC problems for grids and microgrids [9, 10]. For example, relying on a Dynamic Programming (DP) approach, Grillo et al. [11] use a perfect forecast to optimize the control of a non-ideal storage (with a non-linear behavior such as the temperature of the cells and the variation of their resistances). Ramahatana and David [12] use deterministic solar irradiance predictions provided by the ECMWF (European Centre for Medium-Range Weather Forecasts) as input of a DP to optimize the day-ahead operation of an ESS (Energy Storage System) embodied in a microgrid.

The major drawback of deterministic solar forecasts is their nature. Indeed, they are intrinsically uncertain because the weather is a chaotic process. Thus a surge of interest is observed for the probabilistic forecasts, which quantify the uncertainty associated to the predictions [13, 14, 15]. The use of probabilistic forecasts could increase the value of the forecasts for the users. They provide additional information that can be used to improve decision-making. Unlike a binary event such as the rainfall probability, the RES power generation is a continuous variable. More precisely, the probabilistic forecast of an RES is a cumulative distribution function (CDF) that gives the probability associated to the level of production (i.e. power or energy). However, the underlying physics and the economical interpretation of the results of such forecasts are complex to understand. Indeed, the contribution of the probabilistic information is difficult to interpret and the added value to the operation of energy systems is still poorly understood in the domain of smart-grids and grids.

Only a few works deal with the use of probabilistic forecasts of variable RES for the optimization of grid operation. The work of Zhou et al. [16], for example, shows the potential value of probabilistic wind production forecasts in power system operations through construction of scenarios. The forecasts can be incorporated into deterministic UC through probabilistic reserve requirements or can provide scenarios as input to stochastic UC. Furthermore, most of these works propose to associate the uncertainty to a point forecast rather than using the probabilities provided by a probabilistic forecast. The two main methods proposed to take into account the forecasting error are to build scenarios or to use the correlation of the error between the simulation time steps as detailed by Pinson et al. [17]. Alharbi and Raahemifar [18] use the former approach. They build scenarios for the day-ahead schedul-

ing of controllable DG (Distributed Generator) (Wind, PV and storage). In their work, the scenarios are derived from non-realistic forecast errors associated with arbitrarily chosen probabilities. Among others, as presented by Botterud et al. [19, 20], probabilistic forecasts, such as predictions of wind generation quantiles, can be used in reserve sizing or operation to reduce operating cost. For demand-side management, as shown by El-Baz et al. [21, 22], the use of probabilistic solar forecasts can increase the self-sufficiency of a microgrid by 24%. However, in these cases, the selected approach does not capture the effect of the serial correlation of the wind power forecast errors.

Another issue of the UC problem is to handle uncertainties during the optimization process. An important number of stochastic methods exists to solve UC problems as described by Dai et al. [23] or Zheng et al. [24]. The 3 main classes of methods are the SP (Stochastic Programming), the RO (Robust Optimization) and the methods based on the SDP (Stochastic Dynamic Programming). The review of Zhou et al. [25] details techniques and strategies based on stochastic methods applied to the optimization of power system operation in presence of RES. In the field of stochastic optimization, the distributions of the random variables, which corresponds to the inputs of the optimization problem, are generally supposed to be known and the optimization requires the generation of scenarios derived from these distributions. Thus, as showed by Bayraksan and Morton [26] or by Nesterov and Vial [27], the solution of the optimization depends on the sampling techniques used to generate the scenarios, which implicitly relies on the knowledge of the distributions of the random variables. Furthermore, as the actual distributions of the random variables are frequently unknown, a first method proposes to use approximations based on parametric distribution laws such as Beta distribution [28], truncated Normal distribution [29, 30] or Gamma distribution [31]. Another approach relies on historical data, and it is equivalent to use a climatological forecast. Different variants of this approach are discussed by Linderoth et al. [32]. This strategy avoids the need to know the actual distribution. But as stated by Kaut [33] or Shapiro and Nemirovski [34], the long-term trends could not be suitable to represent the near future. As variable RES are very fluctuant, because they result from chaotic weather systems, the use of the climatology as a description of the short-term future is not the best answer. Finally, to the best of our knowledge, it seems that there is no framework to evaluate the effect of the approximation of the input distributions on the quality of the solution obtained by a stochastic optimization.

This work attempts to bridge the gap between the community that develops probabilistic solar forecasts and the one that develops stochastic optimization methods for UC. More precisely, this work proposes a methodology to assess the link between the quality[1] of probabilistic solar forecasts, like the CDF derived from an EPS generated by a NWP, and the results of a stochastic optimization applied to a UC problem. Furthermore, regarding the current state of the art, it is not clear how improving the quality of probabilistic solar forecasts, in terms of improved scores or increased reliability, may lead to added value for the decision-makers. Thus, the goal of this work is two-fold. First, it aims at proposing a method based on the Probabilistic Dynamic Programming (PDP) to integrate probabilistic forecasts of PV production to minimize the operation cost of a microgrid. Second, this work will highlight the opportunity of using probabilistic forecasts instead of deterministic ones to optimally schedule the UC one-day ahead.

A case study based on a real building, an associated PV plant, records of a weather station and operational weather forecasts will serve as support for the proposed methodology. The considered microgrid is composed with a net-zero energy building (NetZeb), Li-ion batteries and a connection to the main grid. The objective is to use day-ahead probabilistic solar forecasts to schedule the commitment of the ESS and to minimize the operation cost of the microgrid.

This work is organized in 4 parts. Section 2 describes the case study and the corresponding data. Section 3 details the microgrid model. Then, section 4 gives an extensive description of the implementation of the probabilistic forecasts inside the optimization framework. Results are discussed in section 5 while section 6 will give some concluding remarks.

2. Case study: Enerpos a NetZeb in the tropics

The considered case study is a NetZeb university building located in Reunion Island [35]. The NetZeb has an annual PV production greater than its energy consumption. Indeed, passive solutions ensure the thermal comfort of the users and a Building Integrated PV (BIPV) farm covers the building needs.

[1]Here, quality refers to the correspondence between the forecasts and the corresponding observations.

2.1. Monitoring system and records

The Enerpos building has a complete monitoring system that records the weather parameters, the electricity consumption and the PV generation. The on-site weather station complies with the WMO standards and records the main weather variables (solar irradiance, dry bulb temperature, relative humidity, rainfall, wind, etc.). Energy meters measure the PV generation and the electricity consumption for the different usages of this educational building: cooling, lights, fans, appliances, lift, etc. The recording time step is of 1 minute for all the parameters and for the considered period (2010-2011). Unfortunately, it is hard to maintain a continuous flow of 1-min measurements and the time-series of data experience an important number of gaps. The consideration of the correlations between the load, the weather and the NWP production is necessary to simulate the microgrid. As a consequence, traditional gap-filling methods, such as interpolation, could not be used in our case. Thus, we built a 2-years time series of 1-min data by aggregating entire days without gaps from the years 2010, 2011 and 2012. The resulting files can be download at [36]. For our case study, hourly averages of the 1-min data have been used. Furthermore, year 2010 will be used to train the calibration procedures described in the next subsection and year 2011 will be used to test the models.

The PV power output is computed from the meteorological data as shown in equation (1). The computation of the PV power output [10] takes into account the global horizontal irradiance (GHI), the ambient temperature (T^a) and the operating characteristics of the PV modules given in Table 1.

$$\begin{aligned} PV_t &= \lambda \times PV^{max} \times \left(\frac{GHI_t}{Ir^{STC}}\right) \times \left(1 - \nu \times \left(T_t^c - T^{c,STC}\right)\right), \\ T_t^c &= \frac{T^a + \left(T^{c,NOCT} - T^{a,NOCT}\right) \times \left(\frac{GHI_t}{Ir^{NOCT}}\right) \times \left(1 - \frac{\eta^{STC} \times \left(1 - \nu \times T^{c,STC}\right)}{\varphi \times \zeta}\right)}{1 + \left(T^{c,NOCT} - T^{a,NOCT}\right) \times \left(\frac{GHI_t}{Ir^{STC}}\right) \times \left(\frac{\nu \times \eta^{STC}}{\varphi \times \zeta}\right)}. \end{aligned} \quad (1)$$

2.2. PV power Forecasts

In this work, we focus on the integration of the PV forecasts in the optimization of the microgrid operation. The future loads of the microgrid (i.e. the different usages of the building) are assumed to be known. Thus, the load forecasts are perfect forecasts corresponding to the measured data. Regarding the solar power generation, 1 deterministic and five probabilistic forecasts

Table 1: PV array characteristics used for the case study

Symbol	Designation	Value	Unit
PV^{max}	Rated capacity of the PV array	6	kW
η^{STC}	Maximum PV efficiency at STC	15.46	%
ν	PV temperature coefficient of power	-0.43	%/°K
T^{a}	Ambient temperature	25	°C
$T^{a,NOCT}$	Ambient temperature at NOCT	20	°C
λ	PV derating factor (wiring losses, shading factor)	95	%
Ir^{STC}	Incident radiation at STC	1	kW
Ir^{NOCT}	Incident radiation at NOCT	0.8	kW
$T^{c,STC}$	PV cell temperature at STC	25	°C
$T^{c,NOCT}$	Nominal operating cell temperature at NOCT	45	°C
φ	Solar transmittance of PV array	90	%
ζ	Solar absorptance of PV array	90	%

from the state of the art will be used, as detailed in Table 2. First, this set of forecasts will allow assessing the improvement brought by the probabilistic approach compared with the deterministic one. Second, we will be able to evaluate the impact of the quality of the forecasts on the value for the users.

The weather forecasts used here are provided by the Ensemble Prediction System of the European Centre of Medium-range Weather Forecasts (ECMWF-EPS) [37]. They consist in up to 10 days ahead of forecasts with a 3-hours granularity. The ECMWF-EPS has 50 members obtained by running 50 times the Integrated Forecasting System (IFS), which is the NWP model used at the ECMWF. Indeed, a small deviation in error analysis can lead to strong differences in the results of the stochastic physics of the atmospheric model. Thus, to take into account uncertainty, initial conditions of the NWP are perturbed and 50 different forecasts are generated simultaneously [38]. Because the raw ECMWF-EPS represents the repartition of the possible outcomes, the sorted members can be interpreted as a set of quantiles of a cumulative distribution function (CDF) [39].

The probabilistic forecast used for the optimization of the grid operation is more precisely the ensemble forecasts generated at midnight with an initial time resolution of 3 hours and a horizon of up to 72 hours. As we plan to optimize the hourly schedule of the storage operation, a down-scaling of the

original ECMWF-EPS is required. The probabilistic forecasts with an hourly granularity are obtained with an oversampling method. The process takes place in two stages:

- Oversampling: The method was developed during the ENDORSE project [40] by the Mines Paristech's team. The method generates a linear interpolation at higher time resolution of the solar irradiance time series assuming energy conservation from shorter to longer samples. It is worth noting that the oversampling procedure can change the order of the EPS members.

- Sorting: The probabilistic forecast, which corresponds to a CDF, is obtained by ordering the M members of the EPS. This commonly used method defines a cumulative distribution function with a probability jump of $1/(M+1)$ between the members. This way to associate the sorted members of the EPS to a CDF is called "uniform" by [39].

The following subsections briefly detail how the other PV power foracasts are generated from this oversampled EPS.

2.2.1. Deterministic forecast

One can easily create a deterministic forecast by taking the mean of the members of the EPS. This deterministic forecast will be referred as "Mean(EPS)". The mean $\widehat{GHI}^{eps}_{t+h}$ in (2) is the average value of the 50 members available at time t and for a forecast horizon h. The mean is considered as the most consistent forecast when the evolution of perturbations in the NWP is nonlinear [38]. However, when the evolution of the perturbations in the model is linear, the mean forecast is almost equal to the deterministic forecast provided by ECMWF. Thus, the mean of the EPS commonly outperforms the control run, and it can be considered as a good challenger of the probabilistic forecasts. This deterministic forecasts reads as

$$\widehat{GHI}^{\overline{eps}}_{t+h} = \frac{1}{M} \sum_{k=1}^{M=50} eps_{t+h,k}. \tag{2}$$

2.2.2. Probabilistic forecasts

In addition to the oversampled EPS derived from the ECMWF-EPS, four probabilistic forecasts will be considered in this work. First, a deseasonalized

climatology $\widehat{GHI}_{t+h}^{Clim}$ is proposed in (4). Its predictive CDF summarized by a set of quantiles with probability levels τ spanning the unit interval is derived from the whole clear sky indices CSI of the training data set sorted in ascending order as given in equation (3). The CSI is the ratio $\frac{GHI}{GHI^{ClearSky}}$ between the measured GHI and the GHI observed under a clear sky. The clear sky irradiances $GHI^{ClearSky}$ required to compute the clear sky indices are provided by the McClear model [41]. The climatology will be used as a reference because it is perfectly reliable and has no resolution (i.e. the forecasted CDF $\widehat{F}(CSI^{train})$ is always the same). The choice to use the CSI for the construction of the climatology is motivated by the elimination of the seasonal and diurnal variation of the GHI along the year. For instance, in winter, a raw climatology based on raw GHI records will misrepresent the possible values of GHI and the higher quantiles will overestimate the occurrence of the GHI outcomes. The equations related to this second probabilistic model are given by

$$\begin{gathered} CSI(\tau) = inf\big\{CSI^{train} \mid \widehat{F}(CSI^{train}) \geq \tau\big\}, \\ \tau \in \{0, 1\}, \end{gathered} \tag{3}$$

and

$$\widehat{GHI}_{t+h}^{Clim}(\tau) = CSI(\tau) \times GHI_{t+h}^{ClearSky}. \tag{4}$$

Second, we use three calibrated ensemble forecasts derived from the oversampled ECMWF-EPS. Indeed, the literature shows that calibration [42] is necessary to increase reliability and consequently the overall quality assessed by proper scores such as the CRPS (see section 2.3). The calibrated forecasts are generated by three different methods namely the Variance Deficit (VD), the analog ensemble, and the Linear Quantile Regression (LQR). These three methods are non-parametric, meaning that there is no need for an *ex-ante* assumption on the characteristics of the forecast distribution.

The variance deficit is a procedure specially designed to answer the lack of variance of the forecast distribution, the most prominent well-known weakness of ensemble forecasts [43]. This is a member-by-member adjustment. It transforms individually each member of an ensemble, in such a way that the calibrated ensemble meets a required condition, i.e. that its variance equals the mean error of the mean of the ensemble. The VD method is exhaustively described by David and Lauret [15].

The second technique used in this study, the LQR, estimates each quantile of the predictive CDF separately. The quantile forecast Q_τ for each

probability level τ is calculated linearly from the mean μ_R and the standard deviation S_R of the raw ensemble and is defined by

$$Q_\tau = \alpha_\tau \times \mu_R + \beta_\tau \times S_R + \gamma_\tau. \tag{5}$$

This formulation implies that both the mean and the variance of the raw ensemble are assumed to be linearly related to the level of the quantile forecasts. The parameters α_τ, β_τ, and γ_τ are calculated by a minimization of the quantile loss function over the training period (see [42] for details).

Finally, the third calibration method is based on the analog ensemble technique which is widely used by the solar forecasting research community [44, 45]. The idea of this method is to associate to a new forecast the closest forecasts in the training period (relatively to some metric). The corresponding measurements of the training period constitute the new ensemble. In this study a very simple method of analog ensemble has been implemented, from the complete procedure explained by Le Gal La Salle et al. [46]. In this version, only the mean of the raw ensemble members is considered as a predictor. It is worth noting the strong differences in the philosophy of the three considered models. When analog ensemble only takes into consideration the mean of the raw ensemble members, linear quantile regression adds the variance to the set of the predictors. Conversely, the variance deficit method considers all the members to build the predictive CDF.

For all the five probabilistic forecasts used in this work, the predictive distributions are given by a set of $M = 50$ discrete quantiles with probabilities spanning the unit interval. In other words, the quantiles range from a probability level of $\tau_1 = 0.02$ to $\tau_{50} = 0.98$ with a step of $\frac{0.98 - 0.02}{50 - 1}$. We chose this distribution of the quantiles to be consistent with the EPS, which has 50 members. Indeed, the EPS can be seen as a CDF with each member corresponding to a quantile and a uniform spacing of the corresponding probabilities (see [39]). The extreme probabilities of 1 and 0 will not be required by the optimization process because their corresponding expectations are null. Indeed, the expectation is the product of the probability with the outcome. And for instance, a probability level of 1 corresponds to an outcome of 0 Wh (i.e at least a production of 0 Wh) and a null probability gives a null expectation.

Table 2: Overview of the 6 solar forecasts considered in this work

Short name	Description	Type
Climatology	Climatological forecast based on the distribution of the clear sky index	Probabilistic (naive)
EPS	Ensemble Prediction System provided by the ECMWF	Probabilistic
Mean(EPS)	Mean of the ECMWF-EPS	Deterministic
LQR	Linear Quantile Regression based on the mean and standard deviation of the ECMWF-EPS	Probabilistic
VD	Variance Deficit applied to the members of the ECMWF-EPS	Probabilistic
ANALOG	Analog Ensemble based on the mean of the ECMWF-EPS	Probabilistic

2.3. Forecast quality

A forecast is characterized by three attributes namely consistency, quality and value [47]. Consistency refers to the agreement between the forecaster's judgement and his forecast. Quality evaluates the correspondence between forecasts and observations. Value quantifies the benefits (economical or others) for the users of the forecasts. In this section, we will detail the main metric defined in the literature that allow assessing both the quality of deterministic and probabilistic forecasts. The value will be addressed through the case study and its computation will be detailed in section 4.

A recent article clearly defines an evaluation framework to carry out a comprehensive assessment of solar probabilistic forecasts [39]. The quality of a probabilistic forecast is characterized by two attributes. First, reliability refers to the statistical consistency between forecasts and observations. Also called calibration, this attribute of the forecast is the most important one. Indeed, non-reliable forecasts would lead to a systematic bias in subsequent decision-making processes [48].

Ensemble calibration can be visually assessed through the use of rank histograms (RH). This graphical tool gives a qualitative assessment of the reliability and it will be used here to characterize the different probabilistic forecasts provided in this work. A RH also gives relevant information about the bias of the forecasts. Their construction is detailed by Lauret et al. [39]. A forecast can be stated as reliable if the histogram of the ranks remains

inside the consistency bands. In the case where statistical consistency is not verified, the different possible other interpretations of a RH are given below. A U-shape RH corresponds to an over-confident probabilistic model (i.e. under-dispersion of the set of forecasts) meaning that the observation is often an outlier in the distribution of forecasts. Conversely, a RH with hump shape means an under-confident model (i.e. distribution of forecasts consistently too large). It indicates that the observation may too often be in the middle of the set of forecasts. Also, asymmetric (or triangle shape) RH is an indication of unconditional forecast biases. Furthermore, overpopulation of the smallest (resp. highest) ranks will correspond to an overforecasting (resp. underforecasting) bias.

Fig. 1 shows the rank histograms of the five considered probabilistic forecasts. As expected, the climatology is perfectly reliable and exhibits a flat rank histogram whose bars remain inside the consistency lines (dotted lines). It is well known that the EPS produces too sharp prediction intervals and the resulting rank histogram has a U-shape, which indicates a lack of spread of the members. The three calibrated forecasts (i.e. LQR, Analog and VD) have a better reliability than the raw EPS. However, the highest rank of the VD and of the LQR is overpopulated and indicates an underforecasting. For these two forecasts we can also observe a bias highlighted by an asymmetric shape of their respective RH. The Analog forecast seems to have the best calibration.

The second attribute is the resolution that measures the ability of a model to generate case dependent forecasts. In other words, a highly resolute forecast is the opposite of the climatological forecast defined in section 2.2.2, which generates a single predictive distribution irrespective of the different forecast situations. A high resolution also ensures sharp prediction intervals. Unfortunately, no visual tool exists to evaluate the resolution. However, the resolution can be quantified by the decomposition of the Continuous Rank Probability Score (CRPS) presented hereafter. The overall quality of a probabilistic forecast can be evaluated with the CRPS [49]. This score is appealing because it corresponds to the mean absolute error (MAE) for a deterministic forecast. It is expressed with the same units as the forecast and it can be decomposed into reliability and resolution. Equation 6 gives the general formulation for a set of N forecast/observation $\{\widehat{F}_j^{fcst}; F_j^{obs}\}$ pairs:

$$\overline{CRPS} = \frac{1}{N}\sum_{j=1}^{N}\int_{-\infty}^{\infty}\left[\widehat{F}_j^{fcst}(x) - F_j^{obs}(x)\right]^2 dx. \tag{6}$$

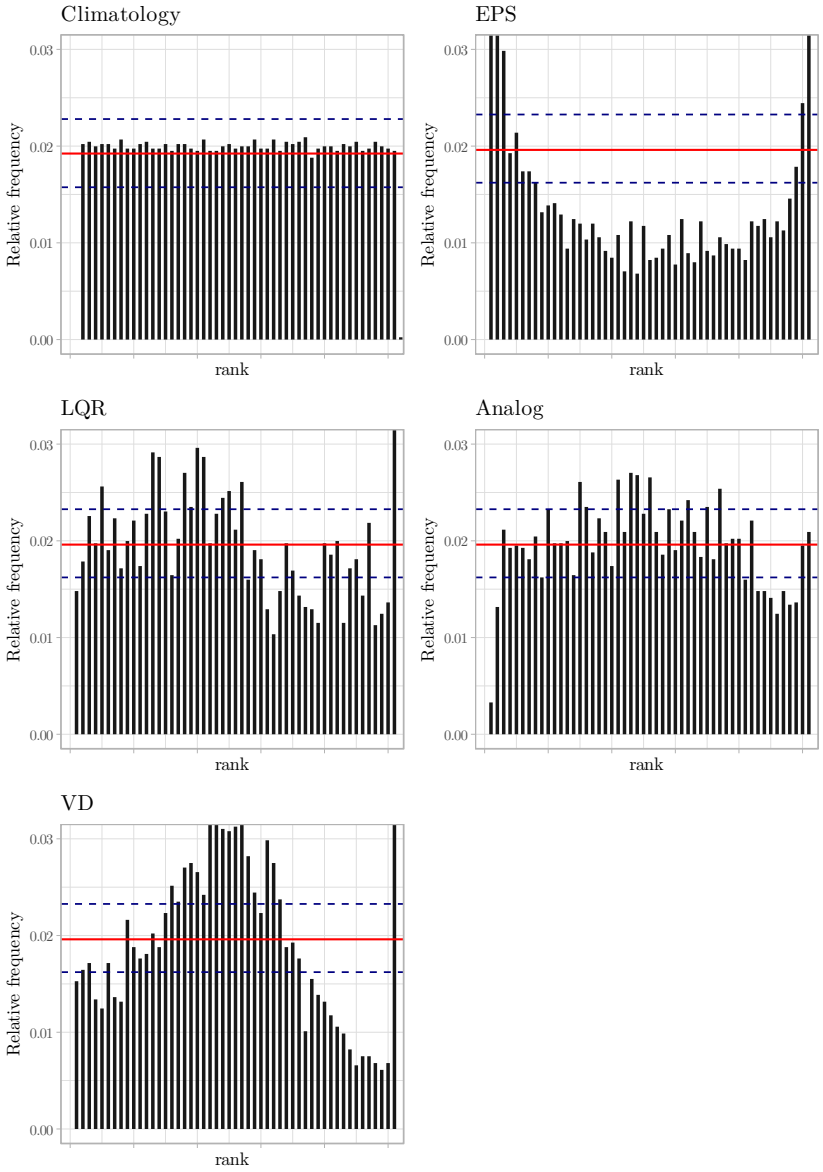

Figure 1: Rank histograms of the five probabilistic forecasts. For sake of clarity, the relative frequency axis has been bound to 3.2%.

To compute the CRPS and its decomposition, we used the R package called "Verification" [50] based on CRPS estimation defined by Gneiting et al.

[42]. Equation (7) gives the CRPS decomposition used in this package and initially proposed by Hersbach [49], where $\overline{Reli}$ is the reliability, $\overline{Resol}$ is the resolution and $\overline{U}$ is the uncertainty, which is a constant term that depends only on the observations. In this work we prefer to use the potential CRPS ($\overline{CRPSpot} = \overline{U} - \overline{Resol}$), also proposed by Hersbach [49]. Indeed, as the uncertainty is constant, the $\overline{CRPSpot}$ is equivalent to the resolution, and it has the advantage to be negatively oriented (lower values are better) like the reliability and the CRPS. The decomposition of the CRPS is given by

$$\overline{CRPS} = \overline{Reli} - \overline{Resol} + \overline{U} = \overline{Reli} + \overline{CRPSpot}. \tag{7}$$

For scores like CRPS that are negatively oriented, the goal of a forecasting model is to minimize as much as possible the $\overline{Reli}$ and the $\overline{CRPSPot}$ terms. In fact, a forecasting model with a high resolution term means that the model has captured the maximum of the variability present in the data (which variability is measured by the uncertainty term). Table 3 shows the CRPS of the five forecasts with their respective decomposition. The decomposition of the deterministic forecasts considered in this work (i.e. Mean(EPS)) is possible. However, the interpretation of the reliability and the resolution of a deterministic forecast is not relevant when compared to probabilistic ones. Thus, the decomposition of the CRPS of the forecast Mean(EPS) is not provided.

The values of the reliability confirm the assessment done with the RH. The Analog forecast has the best reliability, which is equal to the reliability of the Climatology forecast. According to the CRPS, the Analog and the LQR forecasts have the best quality. The relationships between these indicators and the value of the forecasts will be analyzed in detail in section 5.

3. Microgrid model

The considered microgrid is a building load, a building integrated PV (BiPV) farm, an ESS, a connection to the grid and an Energy Management System (EMS) as described in section 1. Energy flows (plain lines) and data transmissions (dashed lines) are illustrated in Fig. 2. The BiPV generation (PV_t), the ESS (ESS_t) and the main grid (Gr_t) are supposed to meet at each time t the load (L_t). However, when there is an excess of production of the microgrid, the energy can be fed into the grid. The balance at time t

Table 3: The CRPS and its decomposition for 6 considered forecasts. For the deterministic forecast Mean(EPS), the CRPS is the MAE.

Models	CRPS (Wh/m^2)	CRPSpot (Wh/m^2)	Reliability (Wh/m^2)
Climatology	70.14	69.86	0.29
EPS	73.61	64.76	8.85
Mean(EPS)	91.89	-	-
LQR	65.86	65.39	0.46
Analog	68.69	68.41	0.29
VD	73.00	70.42	2.57

between the supply and the demand is given by equation (8) hereafter

$$Gr_t + ESS_t + PV_t = L_t. \tag{8}$$

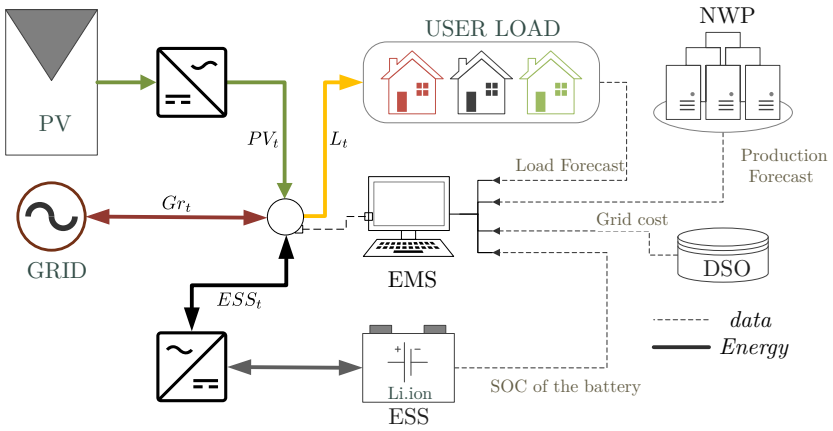

Figure 2: Microgrid energy flows and control diagram

Because the PV farm and the batteries work with direct current (DC) and the building with alternating current (AC), the microgrid has two inverters. Here, we assume that they have the same efficiency curve, defined in equation (9). The inverter efficiency η^{inv} is computed with the model proposed by Riffonneau et al. [10]. The efficiency depends only on the ratio In between the input power and the nominal power of the converter and is defined by

$$\eta^{inv} = \frac{1}{In}(0.0094 + 0.043 \times In + 0.04 \times In^2), \tag{9}$$

The state of charge (SOC) defines the level of energy stored in the ESS. In this work, we assume that the SOC of the ESS can be measured and calculated deterministically. At time t, the SOC depends on the current energy stored in the ESS (Ca_t) and on the nominal capacity Ca_{ref}:

$$SOC_t = \frac{Ca_t}{Ca_{ref}}. \tag{10}$$

Considering a variation ΔSOC_t of the SOC between two time step (t and $t-1$), equation 11 gives the relationships that govern the energy transfers during discharge ($ESS_t^{Discharge} \equiv \Delta SOC_t > 0$) and charge ($ESS_t^{Charge} \equiv \Delta SOC_t < 0$) of the ESS

$$ESS_t = \begin{cases} ESS_t^{Charge} = -\dfrac{\Delta SOC_t \times Ca_{ref}}{\eta^{Charge} \times \eta^{inv,ESS}}, & \text{if } \Delta SOC_t < 0 \\ ESS_t^{Discharge} = \Delta SOC_t \times Ca_{ref} \times \eta^{inv,ESS} \times \eta^{Discharge}, & \text{if } \Delta SOC_t > 0. \end{cases} \tag{11}$$

One can see in this equation that the round trip efficiency of the batteries (η^{ESS}) is distributed between charge and discharge ($\eta^{Charge} = \eta^{Discharge} = \sqrt{\eta^{ESS}}$).

The state of health (SOH) quantifies the level of degradation of the ESS capacity. The SOH variation i.e. ΔSOH is proportional to the SOC variation ΔSOC but only when a discharge occurs. Equation (12) details the degradation model where Z is the aging coefficient that can be derived from the ESS lifetime expressed in number of full cycles and from the corresponding reduction of the state of health of the ESS. The ESS in this study is an lithium iron phosphate battery (LFP). The characteristics of this ESS come from the IRENA cost-of-service tool [51] with reference data from 2020. The full characteristics of the Li-ion batteries used in this work are given in Table 4. The inverter connected to the ESS as a maximum power of 13,5 kW corresponding to 1 C-rate (i.e. 1 capacity of the battery per hour). This relatively low sizing is well suited to our case study because the power of the considered PV field is 6 kWp and the maximum power demand of the building is approximately 7 kW.

$$\begin{aligned} \Delta SOH_t &= Z \times \Delta SOC_{\{\Delta SOC > 0\}}, \\ &= Z \times (SOC_{t-1} - SOC_t)_{\{SOC_{t-1} - SOC_t > 0\}}. \end{aligned} \tag{12}$$

Table 4: Characteristics of the Li-ion batteries considered in the study case

Symbol	Designation	Value	Unit
Ca_{ref}	Storage nominal capacity	13.5	kWh
$ESS_{max}^{Discharge}$	Maximal energy discharge hourly (1C)	13.5	kWh
ESS_{max}^{Charge}	Maximal enrgy charge hourly (1C)	13.5	kWh
SOC_{min}, SOC_{max}	Minimal and maximal state of charge	$10 - 100$	%
SOH_{min}	Minimal state of health	80	%
Z	Ageing coefficient of the storage	8.31^{-5}	
η^{ESS}	Round Trip Efficiency	95.5	%
$P^{inv,ESS}$	ESS Inverter / Chargers rated power	13.5	kW
Sic	Total invest per usable kWh of storage	443.62	€/kWh

4. Optimization problem

As presented by Powell [52], the DP is the best candidate to optimize a computable value function under uncertainty and to solve problems with low dimensions. Furthermore, DP is one of the most successful approach used to solve UC problems [53, 54, 55, 2]. Indeed, the DP is a global optimization methods that works for non-convex and non-linear cost functions. Considering probabilistic solar forecasts as input, a probabilistic version of the DP [56] will be used. In order to avoid going through intermediate processes, such as scenario generation that add more complexity and inaccuracies in the optimization, the choice fell on the direct use of CDF provided by the forecasting models. Thus, we selected the PDP framework to solve a UC problem by taking into account probabilistic forecasts of intermittent RES production.

The aim of the EMS studied in this work is to minimize the operation cost of the microgrid thanks to day-ahead forecasts of the load and of the PV generation. The ESS is the unique controllable device of the system. As a consequence, the objective is to optimize the charging and discharging schedule of the ESS. The following subsections detail the formulation of the optimization problem and how it is implemented in the PDP and in the selected method of reference i.e. SDDP (Stochastic Dual Dynamic Programming) proposed by Pereira and Pinto [57].

4.1. Problem formulation

The objective of the optimization is to minimize the annual operating cost of the microgrid as shown in equation (13). Even if the PV production

is part of the operating cost of the microgrid, it is constant and it will not influence the result of the optimization. As a consequence, the operating cost defined here is the sum of the costs of the storage (R_t) and of the exchanges with the grid ($U_t^{grid} \times Gr_t$).

$$J(SOC) = min \sum_{t=0}^{T} (R_t + U_t^{grid} \times Gr_t) \tag{13}$$

The cost of the storage at time t (R_t) is derived from the aging model proposed by Riffonneau et al. [10]. As stated above, the degradation of the ESS is proportional to the discharged energy. Furthermore, the storage replacement occurs when the minimal state of health SOH_{min} is reached. Thus, the storage cost is computed considering a linear degradation of the capacity due to the aging process as described in the following equation:

$$R_t = \begin{cases} Sic \times Ca_{ref} \times \frac{\Delta SOH_t}{1-SOH_{min}}, & \text{if } SOC_{t-1} - SOC_t > 0 \\ 0, & \text{otherwise,} \end{cases} \tag{14}$$

where SOH_{min} is the minimal state of health of the storage and Sic the storage investment costs obtained from the IRENA projections [51]. Depending on the direction of the energy flow, the grid U_t^{grid} can generate costs or revenues for the microgrid as detailed in equation (15). For the considered case study, the price of electricity (Egp_t) is the sum of the unit cost and of the penalties that depend on hours and seasons [58]. It is worth noting that there is no electricity market in Reunion Island. The prices are fixed by the French national authorities and they are fully known in advance. Furthermore, only the local DSO provides ancillary services and additional incomes by this way are not possible. Table 5 gives an insight of the unit cost of energy and also of the penalties applied in case of overpower. Here, we have set up the power limit at $1kW$ which is the average power demand of the building and corresponds to a peak reduction of a factor of 7. The aim is to significantly reduce the impact of the microgrid on the main grid. Conversely, when the electricity is fed into the grid because the microgrid produces more energy than required, the system generates incomes. In this second case, the electricity is sold to the grid with a constant feed-in-tariff FiT (6.90 c€/kWh) according to the current regulation.

$$U_t^{grid} = \begin{cases} FiT, & \text{if } Gr_t < 0 \\ Egp_t, & \text{if } Gr_t \geq 0. \end{cases} \tag{15}$$

Table 5: Purchased tariff, taxes included, of electricity and penalties applied in case of overpower for the considered study case. All the values are given in c€/kWh.

Designation	Peak	normal		low	
		summer	winter	summer	winter
Unit cost	21.60	11.42	7.38	5.71	5.08
Penalties	1,704.54	715.91	51.14	85.23	34.09

The optimization is subject to 5 constraints. The first one, given by equation (8), is the energy balance of the microgrid . The two following constraints relate to the ESS limitations. The storage capacity in (16) is limited by its minimum and maximum SOC, respectively SOC_{min} and SOC_{max}. Then, if the minimal state of health SOH_{min} is reached (17), the ESS cannot operate anymore and must be replaced. Furthermore, the charge and discharge must not exceed the maximum energy that can flow in and out to the ESS due to the limitation of the power unit (18). The last constraint, given by equation (19), rules the exportation of energy towards the grid ($Gr_t \leq 0$). Indeed, the exportation is allowed only if the microgrid has a excess of production.

$$SOC_{min} \leq SOC_t \leq SOC_{max} \tag{16}$$

$$SOH_t \geq SOH_{min} \tag{17}$$

$$-ESS_{max}^{Charge} \geq ESS_t \leq ESS_{max}^{Discharge} \tag{18}$$

$$Gr_t \leq 0 \quad \text{if} \quad PV_t - L_t + ESS_t^{Discharge} \geq 0 \tag{19}$$

4.2. Dynamic programming (DP)

In the literature, several methods are proposed to optimize the schedule of a microgrid operation. Among these techniques, one can cite Multi-agent algorithms [59, 60, 61, 62], Model Predictive Controller (MPC) optimizer [63, 64, 65] and others [66, 67] that mainly carry out local optimization. The dynamic programming, which allows reaching a global optimum, is also widely used [10, 68, 69, 57]. In this work, we rely on the Hamiltonian Jacobi Bellman equation (HJB) [70] that is a recursive equation depending on the future value of the cost function and on the transition between states.

The definition of the state refers to the work of Bertsekas [71] : "State variable is the minimally dimensioned function of history that is necessary and sufficient to compute the decision function, the transition function, and the contribution function". Thus, the cost function is computed recursively and backward (i.e. $t+1$ toward t) for each state change. The following equation gives the general formulation of DP where the $V_t(S_t)$ is the value of the objective function at time t, depending on the action x_t to reach the state S_t:

$$V_t(S_t) = min\Bigg(C_t(x_t) + \gamma \times \mathbb{E}V_{t+1}(S_{t+1})\Bigg). \tag{20}$$

x_t is the action taken to switch between state t and state $t+1$ from the policy space π. In our case the action is a charge or a discharge of the ESS that respects the maximum and minimum capacity of the ESS. $C_t(x_t)$ is the contribution to the cost of the decision x_t, where C is a function depending on the state at time t and at time $t+1$. Obviously in our case study, S_t and S_{t+1} are the SOC) of the ESS at t and $t+1$ and $\mathbb{E}V_{t+1}(S_{t+1})$ is the expectation of the value for a change between state S_{t+1} and state S_t. Furthermore, x_t corresponds to ESS_t, which is a decision of charge or discharge of the ESS. Finally, γ represents the time value of money. It relates on the weight that a future decision has less influence in the total cost [72]. Considering an infinite horizon, γ is inferior to 1. Because the problem is solved numerically, the state needs to be a real value and will be discretized.

Equation (20) refers to the general formulation of dynamic programming. To take into account the uncertainty associated to the forecasts, two variants of the DP have been proposed: SDP and PDP [56]. Most of the works dealing with grid management use the SDP [10, 68, 73]. For the SDP, many formulations of the Bellman optimal policy are available. For instance, Powell [72] proposed a SDP that uses a stochastic forecast based on a tree search (i.e. a scenario) and roll-out heuristics. Furthermore, the SDP is frequently associated with a Monte Carlo sampling or a Markov Decision process (MDP) [74] to reduce the dimension of the research space and thus to cope with the curse of dimensionality. In this work, we propose to use the PDP algorithm. The HJB equation presented above will not be solved with a Contraction Mapping Point (CMP) [71] method or a differentiation because we assume that the cost-to-go function is not necessarily monotonous or a contraction ($\gamma < 1$). The actual problem is restricted to a 1-dimension problem and it

can be solved directly without any sampling techniques. More precisely, we use the Bellman-Ford [75] backward resolution without space reduction or sampling. This resolution eludes the use of the transition matrix between states, but relies on the known probability distribution of the input data.

4.3. Implementation of the PDP with Probabilistic Forecasts

As a remainder, the objective of this case study is to schedule the SOC of the storage one day ahead. This problem is also called look-ahead policies [72], because we need to solve future problems with the knowledge of future information (forecasts). To take into account events that may occur beyond the first day of operation and that may influence the decisions, we chose to optimize the schedule for the next 3 days but only the first day will be used to operate the ESS. This rolling horizon procedure [76, 5] has been studied extensively for finite or infinite horizon problems.

Furthermore, the storage cost depends only on a decision of discharge (14). As a consequence, the future states of the ESS do not rely on the PV production forecast which is a CDF in our case. This assumption implies that the costs, which are computed by the DP for every possible SOC variations of the ESS, are not probabilistic. In our probabilistic framework, the PV production outcome ($\widehat{PV}$) is a probabilistic distribution of the expected generation. Thus, the grid outcome $\widehat{Gr}$ depends on $\widehat{PV}$ and on the SOC. As a consequence, the apparent cost of a $\{\widehat{PV},\widehat{Gr}\}$ pair is computed for each quantile $\widehat{PV}_{\tau_q}$ of the PV forecast and each possible future SOC of the ESS.

It is important to note that a quantile with a probability level τ_q of a PV forecast namely $\widehat{PV}_{\tau_q}$ corresponds to the minimum value of the PV production that is expected. Indeed, we have a probability τ_q to have a PV production, which corresponds to the quantile $\widehat{PV}_{\tau_q}$, that is the minimum expected value. In our case, we are interested by the contrary event, that is to say the probability to exceed the forecasted quantile, as defined in the following equation:

$$\begin{aligned} Prob(\widehat{PV}_t > \widehat{PV}_{\tau_q}) &= 1 - \tau_q \\ &= 1 - CDF(\widehat{PV}_t). \end{aligned} \tag{21}$$

As the energy balance of the microgrid depends on the variation of storage SOC (i.e. ΔSOC) and on the forecast, the transition between states is implicit. So the probability of transition between states in the general DP

formulation (20) is equal to $p = 1$. As a consequence, the constraint resulting from the energy balance of the microgrid (8) is formulated as follow:

$$\widehat{Gr}_{i,t,q} - ESS_{i,t}^{Charge} + ESS_{i,t}^{Discharge} + \widehat{PV}_{t,\tau_q} = L_t, \tag{22}$$

where i corresponds to the state of the ESS (i.e. the SOC) and $\widehat{Gr}_{i,t,q}$ is the energy exchanged with the grid. As mentioned previously, the SOC is discretized. In our case, we chose a step of discretization of 1%, such as $i \in \{SOC_{min}, SOC_{min} + 0.01, \ldots, SOC_{max}\}$. The predictive CDF of the PV production is also discretized in $M = 50$ quantiles.

The cost-to-go function C_t for the problem is an expectation $\mathbb{E}$ that depends on the probability τ_q to exceed the quantile $\widehat{PV}_{\tau_q}$ given by the PV generation forecasts:

$$\mathbb{E}[C_t(ESS_t)] = R_{i,t} + \frac{1}{M}\sum_{q=1}^{M} \tau_q \times \left(U_t^{grid} \times \widehat{Gr}_{i,t,q}\right), \tag{23}$$

Regarding more precisely the implementation of the deterministic forecast, we simply defined a Heaviside step function with a probability jump of 1 at the forecast value.

Finally, the generated predictive schedule has an 1-hour time step. The receding horizon produces a schedule of the ESS charges and discharges for the next 24 hours based on an optimization done with a horizon of 72 hours. Even if it is possible to adjust online the planning produced by the PDP (e.g. with a MPC), we choose to not do it. Indeed, in this work, we will focus on the performance of the proposed method of optimization. Fig. 3 and 4 show respectively an example of the implementation of the deterministic forecast and of the probabilistic forecast for the same day. In both cases, the ESS runs as scheduled by the lookahead optimization. For the selected day, the deterministic forecast experiences an important overestimation of the PV generation for the second part of the daytime while the probabilistic forecast indicates a significant probability of a lower production in the afternoon. Thus, the fulfillment of the schedule of the ESS obtained with the deterministic forecast results in a purchase of energy from the grid at the end of the afternoon to compensate the error and obviously at a high operating cost. Conversely, the high risk of under-production detected by the probabilistic forecast leads the optimization to slightly discharge the ESS at the end of the afternoon and thus to avoid an important purchase from the grid. As a consequence, the cost of operation is lower.

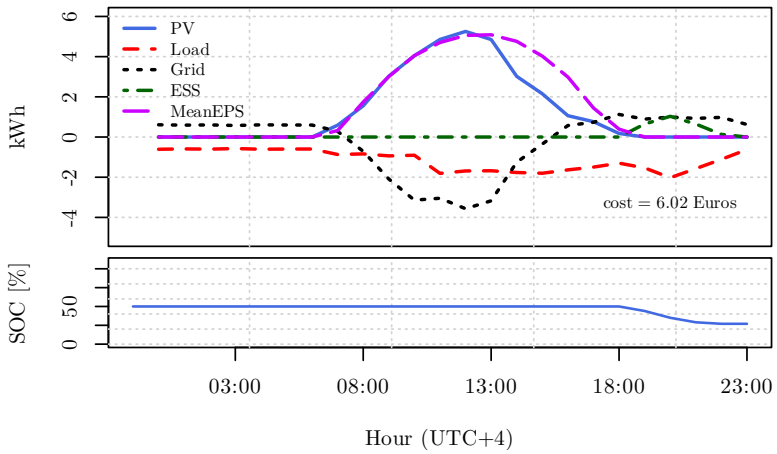

Figure 3: Example of the microgrid operation when using the deterministic forecast to generate the optimal schedule of the ESS. For sake of readability, the load L_t is represented in this figure as a negative quantity.

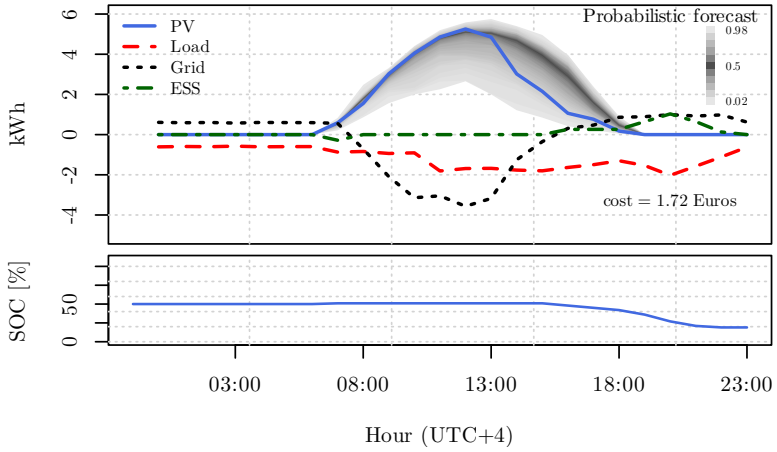

Figure 4: Example of the microgrid operation when using the LQR probabilistic forecast to generate the optimal schedule of the ESS. The grey-scale color shows the quantiles given by the probabilistic forecast. For sake of readability, the load L_t is represented in this figure as a negative quantity.

4.4. Implementation of the reference method: SDDP

To schedule the day-ahead operation of the ESS, we propose to use a well-known stochastic optimization method, i.e. the SDDP, as reference. Here we reproduce the implementation of the SDDP proposed by Kumar et al. [77] that also used a receding horizon. Even if this implementation of the SDDP is close to the one used to implement the PDP some modifications in the problem formulation are required. Indeed, to use the SDDP, the problem must be convex, linear and the objective function has to be positive. To ensure the linearity of the problem, the inverter efficiency (η^{inv}) is fixed to a constant value of 0.9. Furthermore, the state of the system is now the energy stored in the ESS (Ca_t). A change of the state comes from charging and discharging operations and the system cannot do both at the same time:

$$Ca_t = Ca_{t-1} + ESS_t^{Charge} \times \eta^{inv,ESS} \times \eta^{Charge} - \frac{ESS_t^{Discharge}}{\eta^{inv,ESS} \times \eta^{Discharge}}. \quad (24)$$

The constraint resulting from the energy balance (8) of the microgrid becomes:

$$Gr_t - ESS_t^{Charge} + ESS_t^{Discharge} + \overline{PV}_t \times \xi_t = L_t, \quad (25)$$

where the mean PV production ($\overline{PV}_t$) is associated with a perturbation parameter ξ_t that takes the uncertainty into account. Here, the distribution of the historical PV generation (i.e. the training dataset) is used to assess the mean and the uncertainty of the PV production. More precisely, they are both derived from the historical distribution of the clear sky index. Indeed, the clear sky index captures the seasonal variability of the solar resource, which is deterministic, and, in the field of solar energy, distributions derived from clear sky indices are known to outperform the ones directly computed from GHI [78]. Thus, to reproduce the uncertainty of the PV production, the SDDP considered in this work uses the distribution called climatology, which is also used with the PDP and detailed in section 2.2.

The linearization of the constraint relative to the exportation rules (19) is given by the following equation:

$$-Gr_t \leq \begin{cases} ESS_t^{Discharge} + PV_t - L_t, & \text{if} \quad PV_t - L_t \geq 0 \\ ESS_t^{Discharge} - L_t, & \text{otherwise.} \end{cases} \quad (26)$$

To ensure the tractability of the calculation, the sampling method proposed by Shapiro [79] is used to generate a limited number of disturbance

values ξ_t (i.e. scenarios with equal probabilities). It is important to note that the sample size and the sampling technique could influence the solution of the optimization. Tests were carried out with sample size ranging from 50 to 200. For the considered case study, the sample size does not significantly change the resulting operating cost and all the results presented below are obtained for a sample size of 50.

Finally, the SDDP was implemented thanks to the **SDDP.jl** package [80] based on the **JuMP** modeling [81].

5. Results and discussion

5.1. SDDP versus PDP

A comparison of the operating costs obtained with the PDP and the SDDP approaches implemented as detailed above will result in a better performance of the SDDP in all cases (see operating costs given in Tables 6 and 7). Indeed, as illustrated in Fig. 5, the real efficiency of the inverters used in the case study depends on the input power ratio as defined in (9). Thus, the assumption of a constant efficiency of 0.9 done with the SDDP leads to significantly underestimate the losses due to storage charges and discharges. As a consequence the energy flowing through the ESS is overestimated when the input power is lower than 20% of the rated power of the inverter. Finally, as the inverter runs frequently at low input power, the SDDP underestimate the operating cost of the microgrid. This result shows that it is very important to take the non-linearity of the inverters into account to produce relevant optimization results.

However, a fair comparison between the PDP and the well-known stochastic optimization SDDP is required to assess the performance of the methodology proposed in this work. In this subsection, we propose to run the PDP with a constant efficiency of the inverters. Table 6 shows the optimization results for the reference method (i.e. SDDP) and for the proposed PDP approach with this constant efficiency of 0.9 for both approaches. Not all the forecasts associated with the PDP are able to outperform the SDDP. Only the optimizations done with the Analog and LQR forecasts give lower operating cost than the reference method. As the same climatology forecast has been used for both approach, we could expect that the PDP and SDDP results will be fairly close. The difference observed between the two approaches likely results from the control of the ESS done during the online step. Indeed, for the online step of the SDDP, a linear function of the real

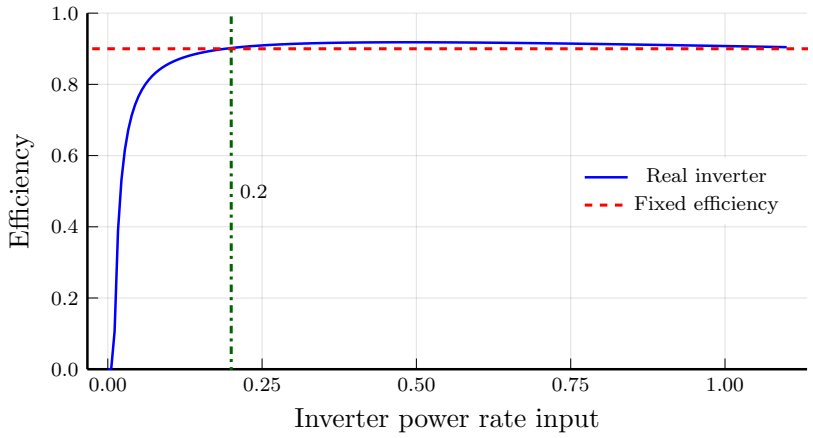

Figure 5: Visual representation of inverter efficiency used for with the PDP (blue line) and with the SDDP (red dashed line)

SOC and of a persistence of the PV production controls the commitment of the ESS. Whereas the PDP predefines the operation of the ESS the day before without any possibility to adjust the planning online.

Table 6: Annual operating obtained with the SDDP (first row) and with the PDP (other rows) costs using a constant efficiency of the inverters for both approaches

Optimization method	Forecasting model	Operating cost €
SDDP	Climatology(CSI)	1587.23
PDP	Perfect	337.81
PDP	Mean(EPS)	2192.46
PDP	EPS	1816.45
PDP	LQR	1525.01
PDP	Climatology(CSI)	1767.77
PDP	VD	1991.87
PDP	Analog	1494.37

5.2. Deterministic versus probabilistic

From an economic point of view, the probabilistic forecasts, even the worst one (i.e. EPS) clearly outperforms the deterministic forecast. Indeed, as illustrated in Table 7, the operating cost of the microgrid (13) obtained

Table 7: Economic and technical annual performance indices [82] of the PDP using a quadratic efficiency curve for the inverters

Forecasting Model	Operating cost €	Autonomy rate %
Perfect	399.87	55.54
Mean(EPS)	3037.67	54.92
EPS	2427.32	56.03
LQR	1889.09	54.67
Climatology	2379.59	49.08
VD	2461.85	53.70
Analog	1966.55	51.97

with the deterministic forecast is reduced by approximately 20% for the worst probabilistic forecast (i.e. EPS) and by 38% for the best ones (i.e. LQR and Analog). Even the climatology, which is a naïve model used in this work as a reference, performs better than the deterministic forecast. Unfortunately, the technical indicator, i.e. the autonomy rate as described by Simpore [82], does not provide relevant information to understand the big gap in terms of operating costs between the probabilistic and deterministic approach.

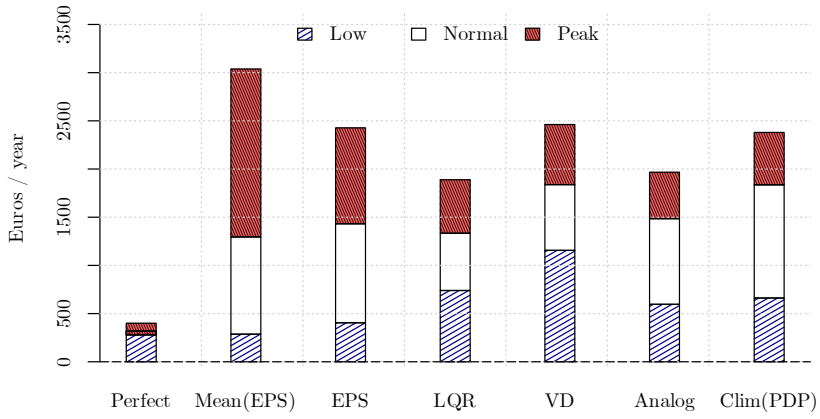

Figure 6: Decomposition by time-of-use rates of the annual cost of the microgrid operation for the PDP results

In Fig. 6, which presents a decomposition of the operating cost by electricity time-of-use rates, we can observe that the perfect forecast purchases

little electricity to the grid and mainly during low hours (i.e. mainly at night). During the daytime, the microgrid is nearly an autonomous system. In the case of the deterministic forecast (Mean(EPS)), the additional operating cost corresponds to the compensation of the forecast errors. These errors are observed only during the normal and peak hours. Obviously, the PV plant produces only on daytime and the low hours occur at night. As a consequence, most of the total cost is normal and peak hours. Using probabilistic forecasts, the EMS tends to counter balance the forecast inaccuracies by purchasing energy mainly during low and normal hours. It allows reducing the overall microgrid demand during peak hours. Finally, as shown in Fig. 7, the costs due to exceeding the power demand constraint (i.e. the penalties) of the electrical grid are considerably reduced with probabilistic forecasts.

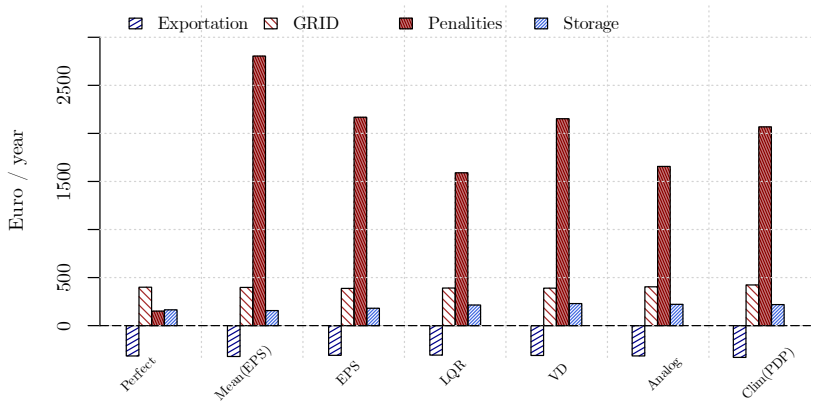

Figure 7: Decomposition of the annual cost of the microgrid operation by type of expense for the PDP results

5.3. Influence of the quality of the forecasts

Several error metrics used to assess the quality of probabilistic and deterministic forecasts exist. All these scores are statistically relevant. However, in the field of solar forecasting, there is no clear framework for choosing the metric which will lead to the best microgrid management. In Table 3, the CRPS of EPS and VD are almost identical (around 73 Wh/m^2) and the microgrid operation cost is almost the same. The VD calibration improves the

reliability of the EPS but decreases the resolution of the forecasts. Thus, the gain in reliability is counterbalanced by the loss in resolution. Regarding the 5 probabilistic forecasts considered in this work, the LQR and Analog methods generate the lowest operating costs.

In Fig. 7, the cost is decomposed by type of expenses (i.e. purchase from the grid, penalties, ESS operation and exportation to the grid). The penalties due to overpower are the most important part of the total cost. Indeed, the selected power limit is restrictive because we chose to reduce at its maximum the impact of the microgrid on the main grid by avoiding high peak power demands. Thus in this study case, the best probabilistic forecast is the one that generates the fewest penalties (i.e. LQR and Analog methods).

One can also note that, except the VD method, the calibration of the EPS leads to forecasts of increased quality and consequently to a better ESS schedule. First, the reliability is significantly improved. Second, the resolution (i.e. CRPSpot) deteriorates. But, the loss in resolution is less important than the gain in reliability. We can conclude that the more efficient methods improves the reliability without deteriorating the resolution.

A sensitivity analysis on the power limit, which is the main cause of the penalties, has been done. When the power limitation is not restrictive, the difference of operating cost observed between the forecasting models is less important. Indeed, the penalties disappear and the cost only depends on the storage operation and on purchases and sales to the grid. But the forecast with the best CRPS still gives the lower operating cost.

6. Conclusion

This work proposes a method for using probabilistic forecasts of intermittent RES, which take the form of discrete quantiles, in order to minimize the operating cost of a microgrid. Our approach combines the probabilistic dynamic programming (PDP) with a receding horizon to solve an optimization problem of scheduling. The PDP can solve linear and non-linear problems and is specifically suitable for the integration of predictive distributions arranged in discrete quantiles. The proposed method has been applied to a microgrid energy management to plan the ESS operation one day ahead. Our case study was a microgrid with a NetZeb building, a BiPV plant and Li-ion batteries.

The comparison between the proposed approached based on the PDP and the well-known SDDP highlights that the consideration of the non-linearity of the converters' efficiency is of paramount importance. Indeed, the chosen implementation of the SDDP, which involves a linearized version of the problem with a constant efficiency of the converters, significantly underestimates the losses and consequently the operation cost.

With the proposed method and for this specific case study, the integration of the probabilistic forecasts in the optimization process results in a more efficient microgrid management and significantly lower operating costs than the use of a deterministic forecast. The probabilistic approach allows anticipating the risk of penalties due to overpower. Indeed, in our case, the power limit is highly restrictive and the operating cost is mainly driven by the penalties.

The approach and tools proposed in this work can be extended to other applications of the EMS in an operational framework. For instance, it can be used for the integration of other intermittent RES, such as wind and wave. However, the study was carried on 1-hour time steps. It will be interesting to test it in real condition with real-time data and a control loop for adjustment and correction.

Acknowledgment

The authors acknowledge the financial support given by Region Reunion and European Regional development Fund (FEDER) under the POE-FEDER 2014-2020 (n°DIRED/20161452-181554) PhD scholarship.

References

[1] B. Saravanan, S. Das, S. Sikri, D. P. Kothari, A solution to the unit commitment problem—a review, Frontiers in Energy 7 (2013) 223–236. doi:10.1007/s11708-013-0240-3.

[2] I. Abdou, M. Tkiouat, Unit Commitment Problem in Electrical Power System: A Literature Review, International Journal of Electrical and Computer Engineering (IJECE) 8 (2018) 1357–1372. doi:10.11591/ijece.v8i3.pp1357-1372.

[3] R. Jiang, J. Wang, Y. Guan, Robust Unit Commitment With Wind Power and Pumped Storage Hydro, IEEE Transactions on Power Systems 27 (2012) 800–810. doi:10.1109/TPWRS.2011.2169817.

[4] IRENA, Electricity storage and renewables: Costs and markets to 2030, International Renewable Energy Agency, Abu Dhabi, 2017. URL: https://www.irena.org/publications/2017/Oct/Electricity-storage-and-renewables-costs-and-markets.

[5] Y. Yang, S. Bremner, C. Menictas, M. Kay, A Mixed Receding Horizon Control Strategy for Battery Energy Storage System Scheduling in a Hybrid PV and Wind Power Plant with Different Forecast Techniques, Energies 12 (2019) 2326. doi:10.3390/en12122326.

[6] H. M. Diagne, P. Lauret, M. David, Solar irradiation forecasting: state-of-the-art and proposition for future developments for small-scale insular grids, in: WREF 2012-World Renewable Energy Forum, 2012, p. . URL: https://hal.archives-ouvertes.fr/hal-00918150/.

[7] J. Antonanzas, N. Osorio, R. Escobar, R. Urraca, F. J. Martinez-de Pison, F. Antonanzas-Torres, Review of photovoltaic power forecasting, Solar Energy 136 (2016) 78–111. doi:10.1016/j.solener.2016.06.069.

[8] S. Sobri, S. Koohi-Kamali, N. A. Rahim, Solar photovoltaic generation forecasting methods: A review, Energy Conversion and Management 156 (2018) 459–497. doi:10.1016/j.enconman.2017.11.019.

[9] A. Tuohy, P. Meibom, E. Denny, M. O'Malley, Unit Commitment for Systems With Significant Wind Penetration, IEEE Transactions on Power Systems 24 (2009) 592–601. doi:10.1109/TPWRS.2009.2016470.

[10] Y. Riffonneau, S. Bacha, F. Barruel, S. Ploix, Optimal Power Flow Management for Grid Connected PV Systems With Batteries, IEEE Transactions on Sustainable Energy 2 (2011) 309–320. doi:10.1109/TSTE.2011.2114901.

[11] S. Grillo, M. Marinelli, S. Massucco, F. Silvestro, Optimal Management Strategy of a Battery-Based Storage System to Improve Renewable Energy Integration in Distribution Networks, IEEE Transactions on Smart Grid 3 (2012) 950–958. doi:10.1109/TSG.2012.2189984.

[12] F. Ramahatana, M. David, Economic optimization of micro-grid operations by dynamic programming with real energy forecast, in: Journal of

Physics: Conference Series, volume 1343, IOP Publishing, EPFL Lausanne, Switzerland, 2019, p. 012067. doi:10.1088/1742-6596/1343/1/012067.

[13] S. Alessandrini, L. Delle Monache, S. Sperati, G. Cervone, An analog ensemble for short-term probabilistic solar power forecast, Applied Energy 157 (2015) 95–110. doi:10.1016/j.apenergy.2015.08.011.

[14] R. Bessa, A. Trindade, C. S. Silva, V. Miranda, Probabilistic solar power forecasting in smart grids using distributed information, International Journal of Electrical Power & Energy Systems 72 (2015) 16–23. doi:10.1016/j.ijepes.2015.02.006.

[15] M. David, P. Lauret, Solar Radiation Probabilistic Forecasting, in: R. Perez (Ed.), Wind Field and Solar Radiation Characterization and Forecasting, Springer International Publishing, Cham, 2018, pp. 201–227. doi:10.1007/978-3-319-76876-2_9.

[16] Z. Zhou, A. Botterud, J. Wang, R. Bessa, H. Keko, J. Sumaili, V. Miranda, Application of probabilistic wind power forecasting in electricity markets, Wind Energy 16 (2012) 321–338. doi:10.1002/we.1496.

[17] P. Pinson, H. Madsen, H. A. Nielsen, G. Papaefthymiou, B. Klöckl, From probabilistic forecasts to statistical scenarios of short-term wind power production, Wind Energy 12 (2009) 51–62. doi:10.1002/we.284.

[18] W. Alharbi, K. Raahemifar, Probabilistic coordination of microgrid energy resources operation considering uncertainties, Electric Power Systems Research 128 (2015) 1–10. doi:10.1016/j.epsr.2015.06.010.

[19] A. Botterud, Z. Zhou, J. Wang, J. Valenzuela, J. Sumaili, R. J. Bessa, H. Keko, V. Miranda, Unit commitment and operating reserves with probabilistic wind power forecasts, in: 2011 IEEE Trondheim PowerTech, 2011, pp. 1–7. doi:10.1109/PTC.2011.6019263.

[20] A. Botterud, Z. Zhou, J. Wang, J. Sumaili, H. Keko, J. Mendes, R. J. Bessa, V. Miranda, Demand Dispatch and Probabilistic Wind Power Forecasting in Unit Commitment and Economic Dispatch: A Case Study of Illinois, IEEE Transactions on Sustainable Energy 4 (2013) 250–261. doi:10.1109/TSTE.2012.2215631.

[21] W. El-Baz, P. Tzscheutschler, U. Wagner, Day-ahead probabilistic PV generation forecast for buildings energy management systems, Solar Energy 171 (2018) 478–490. doi:10.1016/j.solener.2018.06.100.

[22] W. El-Baz, M. Seufzger, S. Lutzenberger, P. Tzscheutschler, U. Wagner, Impact of probabilistic small-scale photovoltaic generation forecast on energy management systems, Solar Energy 165 (2018) 136–146. doi:10.1016/j.solener.2018.02.069.

[23] H. Dai, N. Zhang, Wencong Su, A Literature Review of Stochastic Programming and Unit Commitment, Journal of Power and Energy Engineering 03 (2015) 206. doi:10.4236/jpee.2015.34029, number: 04 Publisher: Scientific Research Publishing.

[24] Q. P. Zheng, J. Wang, A. L. Liu, Stochastic Optimization for Unit Commitment—A Review, IEEE Transactions on Power Systems 30 (2015) 1913–1924. doi:10.1109/TPWRS.2014.2355204.

[25] Z. Zhou, C. Liu, A. Botterud, Stochastic Methods Applied to Power System Operations with Renewable Energy: A Review, Technical Report ANL/ESD-16/14, Argonne National Lab. (ANL), Argonne, IL (United States), 2016. doi:10.2172/1307655.

[26] G. Bayraksan, D. P. Morton, A Sequential Sampling Procedure for Stochastic Programming, Operations Research 59 (2011) 898–913. doi:10.1287/opre.1110.0926.

[27] Y. Nesterov, J. P. Vial, Confidence level solutions for stochastic programming, Automatica 44 (2008) 1559–1568. doi:10.1016/j.automatica.2008.01.017.

[28] J. F. Restrepo, F. D. Galiana, Assessing the Yearly Impact of Wind Power Through a New Hybrid Deterministic/Stochastic Unit Commitment, IEEE Transactions on Power Systems 26 (2011) 401–410. doi:10.1109/TPWRS.2010.2048345.

[29] H. Wu, M. Shahidehpour, Z. Li, W. Tian, Chance-Constrained Day-Ahead Scheduling in Stochastic Power System Operation, IEEE Transactions on Power Systems 29 (2014) 1583–1591. doi:10.1109/TPWRS.2013.2296438.

[30] A. Alabdulwahab, A. Abusorrah, X. Zhang, M. Shahidehpour, Coordination of Interdependent Natural Gas and Electricity Infrastructures for Firming the Variability of Wind Energy in Stochastic Day-Ahead Scheduling, IEEE Transactions on Sustainable Energy 6 (2015) 606–615. doi:10.1109/TSTE.2015.2399855.

[31] A. Turk, Q. Wu, M. Zhang, J. Østergaard, Day-ahead stochastic scheduling of integrated multi-energy system for flexibility synergy and uncertainty balancing, Energy 196 (2020) 117130. doi:10.1016/j.energy.2020.117130.

[32] J. Linderoth, A. Shapiro, S. Wright, The empirical behavior of sampling methods for stochastic programming, Annals of Operations Research 142 (2006) 215–241. doi:10.1007/s10479-006-6169-8.

[33] M. Kaut, Evaluation of scenario-generation methods for stochastic programming, Humboldt-Universität zu Berlin, Mathematisch-Naturwissenschaftliche Fakultät (2003) 14. URL: https://edoc.hu-berlin.de/bitstream/handle/18452/8948/100.pdf?sequence=1.

[34] A. Shapiro, A. Nemirovski, On Complexity of Stochastic Programming Problems, in: V. Jeyakumar, A. Rubinov (Eds.), Continuous Optimization: Current Trends and Modern Applications, Applied Optimization, Springer US, Boston, MA, 2005, pp. 111–146. doi:10.1007/0-387-26771-9_4.

[35] A. Lenoir, F. Garde, Tropical NZEB, High Performing Building Journal (2012) 43–55. URL: https://hal.archives-ouvertes.fr/hal-00918159/.

[36] F. Ramahatana, J. Vigneron, S. Simpore, J. Le Gal La salle, P. Lauret, M. David, EnerPos simulation data, 2020. doi:10.5281/zenodo.4028056, publisher: Zenodo Version Number: 1.

[37] M. Leutbecher, T. N. Palmer, Ensemble forecasting, Journal of Computational Physics 227 (2008) 3515–3539. doi:10.1016/j.jcp.2007.02.014.

[38] A. Persson, F. Grazzini, ECMWF Forecast User Guide, User manual, ECMWF, 2018. URL: https://confluence.ecmwf.int/display/FUG/Forecast+User+Guide.

[39] P. Lauret, M. David, P. Pinson, Verification of solar irradiance probabilistic forecasts, Solar Energy 194 (2019) 254–271. doi:10.1016/j.solener.2019.10.041.

[40] B. Espinar, L. Wald, P. Blanc, C. Hoyer-Klick, Marion Schroedter-Homscheidt, T. Wanderer, Report on the harmonization and qualification of meteorological data, Technical Report 1, Project ENDORSE, Armines, Paris, 2011.

[41] M. Lefèvre, A. Oumbe, P. Blanc, B. Espinar, B. Gschwind, Z. Qu, L. Wald, M. S. Homscheidt, C. Hoyer-Klick, A. Arola, McClear: a new model estimating downwelling solar radiation at ground level in clear-sky conditions, Atmospheric Measurement Techniques 6 (2013) 2403–2418. doi:10.5194/amt-6-2403-2013.

[42] T. Gneiting, A. E. Raftery, A. H. Westveld III, T. Goldman, Calibrated probabilistic forecasting using ensemble model output statistics and minimum CRPS estimation, Monthly Weather Review 133 (2005) 1098–1118. doi:10.1175/MWR2904.1.

[43] T. M. Hamill, Interpretation of Rank Histograms for Verifying Ensemble Forecasts, Monthly Weather Review 129 (2001) 550–560. doi:10.1175/1520-0493(2001)129<0550:IORHFV>2.0.CO;2.

[44] L. D. Monache, F. A. Eckel, D. L. Rife, B. Nagarajan, K. Searight, Probabilistic Weather Prediction with an Analog Ensemble, Monthly Weather Review 141 (2013) 3498–3516. doi:10.1175/MWR-D-12-00281.1.

[45] T. M. Hamill, J. S. Whitaker, Probabilistic Quantitative Precipitation Forecasts Based on Reforecast Analogs: Theory and Application, Monthly Weather Review 134 (2006) 3209–3229. doi:10.1175/MWR3237.1.

[46] J. Le Gal La Salle, J. Badosa, M. David, P. Pinson, P. Lauret, Added-value of ensemble prediction system on the quality of solar irradiance probabilistic forecasts, Renewable Energy 162 (2020) 1321–1339. doi:10.1016/j.renene.2020.07.042.

[47] A. H. Murphy, What Is a Good Forecast? An Essay on the Nature of Goodness in Weather Forecasting, Weather and Forecasting 8 (1993) 281–293. doi:10.1175/1520-0434(1993)008<0281:WIAGFA>2.0.CO;2.

[48] P. Pinson, H. A. Nielsen, J. K. Møller, H. Madsen, G. N. Kariniotakis, Non-parametric probabilistic forecasts of wind power: required properties and evaluation, Wind Energy 10 (2007) 497–516. doi:10.1002/we.230.

[49] H. Hersbach, Decomposition of the Continuous Ranked Probability Score for Ensemble Prediction Systems, Weather and Forecasting 15 (2000) 559–570. doi:10.1175/1520-0434(2000)015<0559:DOTCRP>2.0.CO;2.

[50] M. E. Gilleland, Package 'verification', CRAN, 2015.

[51] IRENA, Electricity storage and renewables: Costs and markets to 2030, Cost-of-service tool, 2017. URL: https://www.irena.org/publications/2017/Oct/Electricity-storage-and-renewables-costs-and-markets.

[52] W. B. Powell, Clearing the Jungle of Stochastic Optimization, in: A. M. Newman, J. Leung, J. C. Smith, H. J. Greenberg (Eds.), Bridging Data and Decisions, INFORMS, 2014, pp. 109–137. doi:10.1287/educ.2014.0128.

[53] P. G. Lowery, Generating Unit Commitment by Dynamic Programming, IEEE Transactions on Power Apparatus and Systems PAS-85 (1966) 422–426. doi:10.1109/TPAS.1966.291679.

[54] W. L. Snyder, H. D. Powell, J. C. Rayburn, Dynamic Programming Approach to Unit Commitment, IEEE Transactions on Power Systems 2 (1987) 339–348. doi:10.1109/TPWRS.1987.4335130.

[55] Z. Ouyang, S. Shahidehpour, An intelligent dynamic programming for unit commitment application, IEEE Transactions on Power Systems 6 (1991) 1203–1209. doi:10.1109/59.119267.

[56] W. L. Winston, Operations Research: Applications and Algorithms, 4 ed., Duxbury Press, Belmont, Calif., 2003. URL:

https://itslearningakarmazyan.files.wordpress.com/2015/09/operation-research-aplications-and-algorithms.pdf.

[57] M. V. F. Pereira, L. M. V. G. Pinto, Multi-stage stochastic optimization applied to energy planning, Mathematical Programming 52 (1991) 359–375. doi:10.1007/BF01582895.

[58] EDF Reunion, Tarifs et catalogues de prestations, 2018. URL: https://reunion.edf.fr/entreprises/decouvrir-nos-tarifs-et-services/tarifs-et-catalogues-de-prestations-2.

[59] A. Dimeas, N. Hatziargyriou, Operation of a multiagent system for microgrid control, IEEE Transactions on Power Systems 20 (2005) 1447–1455. doi:10.1109/TPWRS.2005.852060.

[60] T. Logenthiran, D. Srinivasan, A. M. Khambadkone, H. N. Aung, Multiagent System for Real-Time Operation of a Microgrid in Real-Time Digital Simulator, IEEE Transactions on Smart Grid 3 (2012) 925–933. doi:10.1109/TSG.2012.2189028.

[61] C.-X. Dou, X.-B. Jia, H. Li, M.-F. Lv, Multi-agent System Based Energy Management of Microgrid on Day-ahead Market Transaction, Electric Power Components and Systems 44 (2016) 1330–1344. doi:10.1080/15325008.2016.1158216.

[62] J. Achara, M. Mohiuddin, W. Saab, R. Rudnik, J.-Y. Le Boudec, T-RECS: A software testbed for multi-agent real-time control of electric grids, in: 2017 22nd IEEE International Conference on Emerging Technologies and Factory Automation (ETFA), IEEE, Limassol, 2017, pp. 1–4. doi:10.1109/ETFA.2017.8247706.

[63] M. Zachar, P. Daoutidis, Nonlinear Economic Model Predictive Control for Microgrid Dispatch, IFAC-PapersOnLine 49 (2016) 778–783. doi:10.1016/j.ifacol.2016.10.260.

[64] G. Bruni, S. Cordiner, V. Mulone, V. Sinisi, F. Spagnolo, Energy management in a domestic microgrid by means of model predictive controllers, Energy 108 (2016) 119–131. doi:10.1016/j.energy.2015.08.004.

[65] M. Arnold, G. Andersson, Model predictive control of energy storage including uncertain forecasts, in: Power Systems Computation Conference (PSCC), Stockholm, Sweden, volume 23, Citeseer, 2011, pp. 24–29. URL: http://citeseerx.ist.psu.edu/viewdoc/download?doi=10.1.1.722.6663&rep=rep1&type=pdf.

[66] B. Zhao, Y. Shi, X. Dong, W. Luan, J. Bornemann, Short-Term Operation Scheduling in Renewable-Powered Microgrids: A Duality-Based Approach, IEEE Transactions on Sustainable Energy 5 (2014) 209–217. doi:10.1109/TSTE.2013.2279837.

[67] E. C. Umeozor, M. Trifkovic, Operational scheduling of microgrids via parametric programming, Applied Energy 180 (2016) 672–681. doi:10.1016/j.apenergy.2016.08.009.

[68] M. Y. Nguyen, Y. T. Yoon, N. H. Choi, Dynamic programming formulation of Micro-Grid operation with heat and electricity constraints, in: 2009 Transmission Distribution Conference Exposition: Asia and Pacific, 2009, pp. 1–4. doi:10.1109/TD-ASIA.2009.5356870.

[69] N. A. Luu, Q.-T. Tran, S. Bacha, Optimal energy management for an island microgrid by using dynamic programming method, in: 2015 IEEE Eindhoven PowerTech, 2015, pp. 1–6. doi:10.1109/PTC.2015.7232678.

[70] D. P. Bertsekas, Dynamic programming and optimal control, volume 1 of *Athena scientific optimization and computation series*, 4 ed., Athena scientific, Belmont, Massachusetts, 1995. URL: http://athenasc.com/dpbook.html.

[71] D. P. Bertsekas, Dynamic Programming and Stochastic Control, number 125 in Mathematics in Science and Engineering, Academic Press, New York, San Francisco and London, 1976.

[72] W. B. Powell, Approximate Dynamic Programming: Solving the Curses of Dimensionality, John Wiley & Sons, 2011. doi:10.1002/9781118029176.

[73] F. Borghesan, Approximate dynamic programming techniques for microgrid energy management, PhD Thesis, Polytechnic University of Milan, Milan, 2013. URL: https://www.politesi.polimi.it/bitstream/10589/78475/3/Tesi_inglese%20con%20frontespizio.pdf.

[74] M. L. Puterman, Markov Decision Processes: Discrete Stochastic Dynamic Programming, Wiley Series in Probability and Statistics, John Wiley & Sons, Ltd, 1994. doi:10.1002/9780470316887.

[75] B. V. Cherkassky, A. V. Goldberg, T. Radzik, Shortest paths algorithms: Theory and experimental evaluation, Mathematical Programming 73 (1996) 129–174. doi:10.1007/BF02592101.

[76] S. Chand, V. N. Hsu, S. Sethi, Forecast, Solution, and Rolling Horizons in Operations Management Problems: A Classified Bibliography, Manufacturing & Service Operations Management 4 (2002) 25–43. doi:10.1287/msom.4.1.25.287.

[77] R. Kumar, M. J. Wenzel, M. J. Ellis, M. N. ElBsat, K. H. Drees, V. M. Zavala, A Stochastic Dual Dynamic Programming Framework for Multiscale MPC, IFAC-PapersOnLine 51 (2018) 493–498. doi:10.1016/j.ifacol.2018.11.041.

[78] J. Le Gal La Salle, M. David, P. Lauret, A new climatology reference model to benchmark probabilistic solar forecasts, Solar Energy 223 (2021) 398–414. doi:10.1016/j.solener.2021.05.037.

[79] A. Shapiro, Monte Carlo Sampling Methods, in: Handbooks in Operations Research and Management Science, volume 10, Elsevier, 2003, pp. 353–425. doi:10.1016/S0927-0507(03)10006-0.

[80] O. Dowson, L. Kapelevich, SDDP.jl : A Julia Package for Stochastic Dual Dynamic Programming, INFORMS Journal on Computing (2020) ijoc.2020.0987. doi:10.1287/ijoc.2020.0987.

[81] I. Dunning, J. Huchette, M. Lubin, JuMP: A Modeling Language for Mathematical Optimization, SIAM Review 59 (2017) 295–320. doi:10.1137/15M1020575.

[82] S. Simpore, Modélisation, simulation et optimisation d'un système de stockage à air comprimé couplé à un bâtiment et à une production photovoltaïque, Ph.D. thesis, Université de La Réunion, 2018. URL: https://tel.archives-ouvertes.fr/tel-02059339.